Theoret. Comput. Fluid Dynamics (2002) 16: 59–69
Digital Object Identifier (DOI) 10.1007/s00162-002-0065-x

Theoretical and Computational Fluid Dynamics

Modulated Taylor–Couette Flow: Onset of Spiral Modes*

J.M. Lopez

Department of Mathematics and Statistics, Arizona State University,
P.O. Box 871804, Tempe, AZ 85287-1804, U.S.A.
lopez@math.asu.edu

F. Marques

Department of Applied Physics, Universitat Politècnica de Catalunya,
08034 Barcelona, Spain
marques@fa.upc.es

Communicated by H.J.S. Fernando

Received 5 November 2001 and accepted 29 March 2002
Published online 2 October 2002 – © Springer-Verlag 2002

Abstract. The linear stability of the flow between concentric cylinders, with the inner cylinder rotating at a constant angular velocity and the outer cylinder with an angular velocity varying harmonically about a zero mean, is addressed. The bifurcations of the base state are analyzed using Floquet theory, paying particular attention to non-axisymmetric bifurcations which are dominant in significant regions of parameter space. In these regions the spiral modes of the unforced system become parametrically excited and dominant. This is typical behavior of parametrically forced extended systems, where some modes are stabilized, but others are simultaneously excited. The flow structure of the bifurcated states are examined in detail, paying particular attention to the dynamic implications of their symmetries, and in particular how and when subsequent period doublings are inhibited.

1. Introduction

Temporally forced Taylor–Couette flow has been a paradigm problem for the parametric control of flow instability by temporal forcing. There have been two fundamentally different ways that temporal forcing has been imparted to the system. The first consists of harmonically modulated rotations of either the inner or outer cylinder; we refer to this class of flows as modulated Taylor–Couette, MTC. The other class consists of harmonic oscillations of the inner cylinder in the axial direction; oscillatory Taylor–Couette, OTC. The two are shown schematically in Figure 1. Whereas OTC has always been found to be stabilizing (Hu and Kelly, 1995; Weisberg *et al.*, 1997; Marques and Lopez, 1997, 2000), for MTC both experiments and theoretical investigations (Donnelly *et al.*, 1962; Donnelly, 1964; Carmi and Tustaniwskyj, 1981; Walsh *et al.*, 1987; Walsh and Donnelly, 1988; Barenghi and Jones, 1989; Murray, *et al.*, 1990; Barenghi, 1991; Ganske *et al.*, 1994) have shown that under differing combinations of mean state and temporal forcing, the onset of instability may be enhanced or delayed compared with the unforced system. Regardless of the particulars of the

* This work was supported by NSF Grants INT-9732637 and CTS-9908599 (U.S.A.) and MCYT Grants PB97-0685 and BFM2001-2350 (Spain).

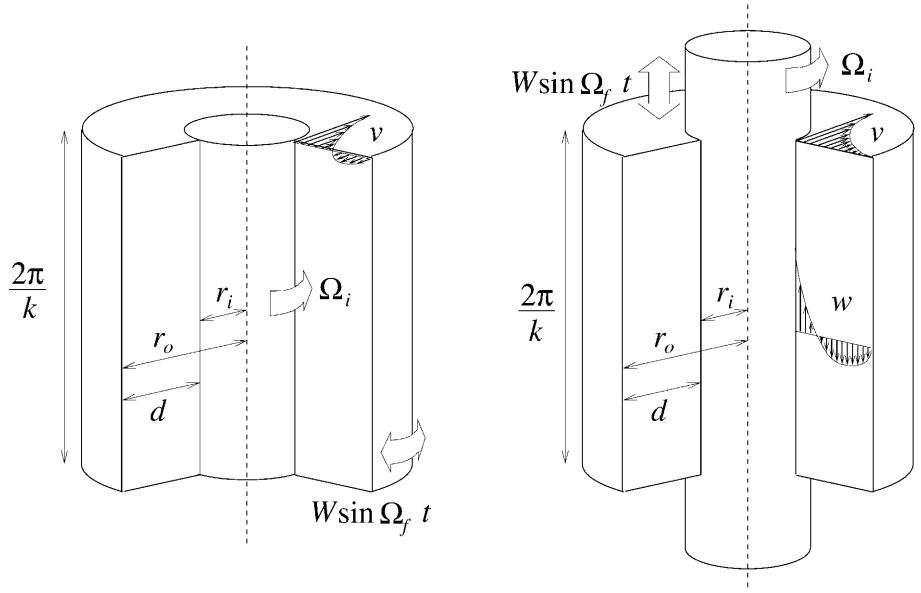

Figure 1. Schematics of temporally forced Taylor–Couette; (a) outer cylinder oscillating azimuthally, MTC, and (b) inner cylinder oscillating axially, OTC.

MTC problem, there has been overwhelming discussion in the literature concerning discrepancies between experiments and stability analysis at the lower end of the range of forcing frequencies considered. A number of possible explanations have been put forward, e.g., nonlinear transitions due to low frequency forcing allowing eigenmodes to grow beyond linear limit, and imperfections (Barenghi and Jones, 1989; Barenghi, 1991), but none of these has been systematically investigated and shown to be able to account for the discrepancies. On the theoretical side, it is apparent that for most studies only axisymmetric disturbances have been considered, and yet a number of experiments (Tennakoon *et al.*, 1997) have observed the onset of instability to non-axisymmetric modes in some parameter regimes. In contrast, the OTC problem has found excellent agreement between experiments and theory (once the presence of endwalls are accounted for to lowest order), including the onset of non-axisymmetric states when the forcing frequency is of the order of the precession frequency of the spiral modes in the unforced system (Sinha and Smits, 2000). This motives a re-examination of the MTC problem, allowing for non-axisymmetric perturbations.

Of any variants of MTC, in this paper we consider the linear stability of the flow between concentric cylinders with the inner cylinder rotating at a constant angular velocity and the outer cylinder with an angular momentum which is sinusoidal about a zero mean. For this configuration, Donnelly's group (Walsh and Donnelly, 1988) found that the modulation of the outer cylinder delayed the onset of instability to higher rotation rates of the inner cylinder compared with the zero-modulation case. Theoretical treatments of this flow (Carmi and Tustaniwskyj, 1981; Barenghi and Jones, 1989; Murray *et al.*, 1990) have been unable to obtain reasonable agreement with the experiments in the low frequency large amplitude modulation regime. Here, we present a Floquet analysis of the time-periodic basic state that considers axisymmetric and non-axisymmetric perturbation modes, and allows for variable axial wave numbers; these two features have not been considered in all previous studies. The non-axisymmetric perturbations lead to Neimark–Sacker bifurcations, Hopf bifurcations from limit cycles, and then the time integration for the monodromy matrix needs to allow for quasiperiodic bifurcated states.

2. Implications of the Symmetries on the Dynamics

The symmetry group of the Taylor–Couette problem without periodic forcing is O(2) $\times$ SO(2) (e.g., see Chossat and Iooss, 1994). O(2) consists of translations in the axial direction, where axial periodicity is assumed, and the axial reflection R: $z \to -z$. The SO(2) comes from rotations around the axis. In the period-

ically forced case, the symmetry group is still O(2) × SO(2), but the physical realization of O(2) is different in MTC and OTC; axial translations and rotations continue to be symmetries of both temporally forced systems. In the case of azimuthal oscillations, MTC, the governing equations are invariant with respect to the axial reflection R, as in the unforced case. However, due to the axial oscillations in OTC, the axial reflection is no longer a symmetry of the problem, but composing it with a half-period time translation we obtain a time-gliding symmetry G of the system. This symmetry, together with axial translations, still gives the symmetry group O(2). The explicit expression of this symmetry, acting on the velocity field, is

$$(G(u, v, w))(r, \theta, z, t) = (u, v, -w)(r, \theta, -z, t + T/2)\,. \tag{1}$$

The main difference between the MTC and OTC cases is that in MTC the R symmetry is purely spatial, whereas in OTC it is a space–time symmetry. The implications of this is that the two basic states follow different bifurcation scenarios.

The stability of the basic state is determined by Floquet analysis, where the Navier–Stokes equations are linearized about the basic state, the linear system with a complete basis for general perturbations is evolved for a forcing period, and the eigenvalues of the resulting monodromy matrix are examined. Change of stability occurs when one or more eigenvalues have unit modulus; this can occur in three generic ways. In the first, the critical eigenvalue μ crosses the unit circle through $+1$, a synchronous bifurcation; in the second, μ crosses through -1, a subharmonic bifurcation. The third way is for a pair of complex conjugate eigenvalues to cross, $\mu_{1,2} = \mathrm{e}^{\pm \mathrm{i}\phi}$, a Neimark–Sacker bifurcation. The presence of the Z_2 symmetry subgroups generated by R and G may alter this generic scenario. In the case of MTC, the basic state limit cycle is invariant to a purely spatial Z_2 symmetry, and the standard bifurcation theory (Kuznetsov, 1998) shows that the bifurcation follows the generic scenario, and in particular period doublings ($\mu = -1$) are allowed. In the case of OTC, the presence of a space–time Z_2 symmetry generated by G implies that the Poincaré map of the basic state limit cycle is the square of another map, inhibiting period doubling via a simple eigenvalue $\mu = -1$ (Swift and Wiesenfeld, 1984; Marques and Lopez, 2000). In neither case are there restrictions on the Neimark–Sacker bifurcation ($\mu = \mathrm{e}^{\pm \mathrm{i}\phi}$). In fact, the breaking of the $SO(2)$ azimuthal symmetry generically gives a Neimark–Sacker bifurcation to a modulated rotating wave, where the precession frequency is given by ϕ and the modulation comes from the temporally forced basic state. Note that Neimark–Sacker bifurcations are inhibited in very low-dimensional systems (dim ≤ 3, see Kuznetsov (1998)), as is the case in the two-dimensional Mathieu equation which has been the standard model used in parametric resonance studies (clearly, the discretized Taylor–Couette problems are of large dimension).

3. Description of the MTC Case

We consider the flow between two concentric cylinders of infinite length, inner and outer radii r_i and r_o, and gap $d = r_\mathrm{o} - r_\mathrm{i}$. The inner cylinder is rotating constantly, at Ω_i rad/s, while the outer cylinder oscillates about a zero mean at $\Omega_\mathrm{o} = \epsilon\Omega_\mathrm{i} \cos \omega t$ rad/s. The governing parameters are the inner Reynolds number, $Ri = \Omega_\mathrm{i} r_\mathrm{i} d/\nu$, the radius ratio, $\eta = r_\mathrm{i}/r_\mathrm{o}$, the forcing amplitude ratio, ϵ, and the forcing frequency, ω, where ν is the kinematic viscosity. The length scale used is the gap, d, and the diffusive time across the gap, d^2/ν, is the time scale.

The basic state is time periodic, the radial and axial velocity components are zero, and the azimuthal velocity component depends only on (r, t). This azimuthal component v_b is the sum of two terms, the well-known Couette flow

$$v_\mathrm{TC}(r) = \frac{r_\mathrm{i} r_\mathrm{o}}{r_\mathrm{o}^2 - r_\mathrm{i}^2} \left(\frac{r_\mathrm{o}}{r} - \frac{r}{r_\mathrm{o}} \right) Ri, \tag{2}$$

and a periodic component $v_\mathrm{p}(r, t)$. The Navier–Stokes equations for $v_\mathrm{p} = (\epsilon Ri/\eta)\mathrm{Real}(F(r)\mathrm{e}^{\mathrm{i}\omega t})$ reduce to

$$F'' + \frac{1}{r} F' - \left(\mathrm{i}\omega + \frac{1}{r^2} \right) F = 0, \qquad F(r_\mathrm{i}) = 0, \quad F(r_\mathrm{o}) = 1. \tag{3}$$

The solution is a linear combination of the modified Bessel functions of order one, $I_1(y)$, $K_1(y)$, with complex argument $y = \omega^{1/2} r e^{i\pi/4}$ (Murray *et al.*, 1990):

$$f(r) = \begin{vmatrix} I_1(y) & K_1(y) \\ I_1(y_o) & K_1(y_o) \end{vmatrix} \Big/ \begin{vmatrix} I_1(y_i) & K_1(y_i) \\ I_1(y_o) & K_1(y_o) \end{vmatrix}, \tag{4}$$

where y_i and y_o are the values of y at $r = r_i$ and r_o, respectively.

The linear stability of the basic state is determined by Floquet analysis following Marques and Lopez (1997). We perturb the basic state by a small disturbance which is assumed to vary periodically in the azimuthal and axial directions:

$$\mathbf{v}(r, \theta, z, t) = \mathbf{v}_b(r, t) + e^{i(n\theta + kz)} \mathbf{u}(r, t); \tag{5}$$

the boundary conditions for $\mathbf{u}$ are homogeneous, $\mathbf{u}(r_i) = \mathbf{u}(r_o) = \mathbf{0}$. Linearizing the Navier–Stokes equations about the basic solution, we obtain a linear system for the perturbation $\mathbf{u}$ with time-periodic coefficients.

The system is discretized in space using a Petrov–Galerkin scheme. The velocity field $\mathbf{u}$ is expanded in a suitable solenoidal basis satisfying the boundary conditions,

$$\mathbf{u} = \sum_j a_j \mathbf{u}_j, \tag{6}$$

and the linearized equations are projected onto a different solenoidal basis $\tilde{\mathbf{u}}_j$, satisfying the boundary conditions. A comprehensive analysis of the method can be found in Moser *et al.* (1983) and Canuto *et al.* (1988). After projection, the pressure term disappears, and we get a system of ordinary differential equations for the coefficients a_j:

$$\mathbf{G}\dot{\mathbf{x}} = \mathbf{H}(t)\mathbf{x} = (\mathbf{A} + \mathbf{B}\sin\omega t + \mathbf{C}\cos\omega t)\mathbf{x}, \tag{7}$$

where the vector $\mathbf{x}$ contains the real and imaginary parts of the coefficients a ($a_j = x_{2j-1} + i x_{2j}$), and the matrices $\mathbf{A}$, $\mathbf{B}$, $\mathbf{C}$, $\mathbf{G}$ are time independent, with $\mathbf{G}$ positive definite (see Marques and Lopez (1997) for details). A second-order implicit trapezoidal method is used for time integration, with a time step that depends on the number of modes, the inner Reynolds number Ri, the modulation amplitude ϵ, and the modulation frequency ω. The fundamental matrix of (7) is the solution of the system

$$\mathbf{G}\dot{\mathbf{X}} = \mathbf{H}(t)\mathbf{X}, \qquad \mathbf{X}(0) = \mathbf{I}, \tag{8}$$

where $\mathbf{I}$ is the identity matrix, whose columns form a basis of the disturbances x. Integrating over a forcing period $T = 2\pi/\omega$, we obtain the monodromy matrix of the system $\mathbf{X}(T)$, whose eigenvalues μ_j, called Floquet multipliers, control the growth rate of the perturbations.

The velocity field in the linearized problem depends on (θ, z) in a simple way, through the combination $n\theta + kz$. Therefore, the θ and z derivatives are proportional, $\partial_\theta = (n/k)\partial_z$. The incompressibility condition is

$$\partial_r(ru) + \partial_z\left(\frac{n}{k}v + rw\right) = 0. \tag{9}$$

This allows the introduction of a generalized streamfunction ψ satisfying

$$\partial_z\psi = -ru, \qquad \partial_r\psi = \frac{n}{k}v + rw. \tag{10}$$

Introducing the axial component of the angular momentum, $\gamma = rv$, as is usual in axisymmetric problems, the velocity components are given in terms of ψ, γ as follows:

$$u = -\frac{1}{r}\partial_z\psi, \qquad v = \frac{1}{r}\gamma, \qquad w = \frac{1}{r}\partial_r\psi - \frac{n}{kr^2}\gamma. \tag{11}$$

Notice that in the axisymmetric case $n = 0$, ψ reduces to the Stokes streamfunction, contours of ψ in the (r, z) plane are streamlines, and contours of γ are vortex lines. In the general case with $n \neq 0$, the (instantaneous) streamlines lay on ψ isosurfaces, and these surfaces are invariant to the helical symmetries $\theta \to \theta + \beta$,

$z \to z - n\beta/k$ for all β. Therefore, contours of ψ, γ in the (r, z) plane give a fairly complete description of the flow also in the general case, and we present our results in this way.

A convenient expansion basis, inspired by (11), is given by

$$\mathbf{u}_{2j-1} = (f_j, 0, \mathrm{i}\partial_r(rf_j)/(kr)), \qquad \mathbf{u}_{2j} = (0, g_j, -ng_j/(kr)). \tag{12}$$

The boundary conditions for f_j and g_j, obtained from the homogeneous boundary conditions for $\mathbf{u}_j$, are $f_j = f_j' = g_j = 0$ at $r = r_\mathrm{i}, r_\mathrm{o}$. Introducing the new radial coordinate $y = 2(r - r_\mathrm{i})/d - 1$, $y \in [-1, +1]$, and using Chebyshev polynomials T_j, a simple choice for f_j and g_j, which satisfy the homogeneous boundary conditions, is

$$f_j(r) = \big(1 - y^2\big)^2 T_{j-1}(y), \qquad g_j(r) = \big(1 - y^2\big) T_{j-1}(y), \tag{13}$$

where $j \in [1, M]$, and M is the number of Chebyshev polynomials used. In order to preserve the orthogonality relationships between the Chebyshev polynomials, and to avoid $1/r$ factors in the inner products appearing in the matrices $\mathbf{A}$, $\mathbf{H}$, a suitable choice for the projection basis $\tilde{\mathbf{u}}$ is

$$\tilde{f}_j(r) = r^3\big(1 - y^2\big)^{3/2} T_{j-1}(y), \qquad \tilde{g}_j(r) = r^3\big(1 - y^2\big)^{1/2} T_{j-1}(y), \tag{14}$$

differing from the expansion basis $\mathbf{u}$ only in the factor $r^3(1 - y^2)^{-1/2}$. With this choice, most of the inner products involve polynomials, and can be numerically computed exactly using Gauss–Chebyshev quadrature; see Marques and Lopez (2000) for further details.

Functions f and g are associated with the generalized streamfunction and the azimuthal velocity, respectively. The expressions of ψ, γ in term of f, g and the coefficients x of the velocity field expansion can be obtained after some algebra, and are

$$\psi = -\sum_{j=1}^{M} \big(x_{4j-3}(t)\sin(n\theta + kz) + x_{4j-2}(t)\cos(n\theta + kz)\big)\frac{r}{k} f_j(r), \tag{15}$$

$$\gamma = \sum_{j=1}^{M} \big(x_{4j-1}(t)\cos(n\theta + kz) - x_{4j}(t)\sin(n\theta + kz)\big) r g_j(r). \tag{16}$$

Convergence: The spectrum of the continuous system ($M \to \infty$) has an accumulation point at $\mu = 0$, and only a finite (usually small) number of eigenvalues are far from zero and approach the unit circle in the complex plane. We are interested in the most dangerous eigenvalue, with maximum modulus. When it crosses the unit circle, the base state becomes unstable. This eigenvalue can be computed with great accuracy using a small number of terms in the expansion (6). We have found that the critical Ri and k can be determined to one part in ten thousand using $M = 10$ modes. If one were interested in additional eigenvalues, particularly those close to the origin, a much larger number of modes should be used.

4. Results

We present results for three radius ratios, $\eta = 0.88$, 0.719 (considered previously by others), and 0.5; the forcing amplitude ratio in all three cases is $\epsilon = 1.5$, as in previous studies. Figure 2 summarizes the variation of Ri_crit and k_crit with ω. Comparing these values with the critical Ri and k in the unforced case ($\epsilon = 0$, the usual Taylor–Couette system), given in Table 1, two basic features emerge. First, the azimuthal modulation produces a large stabilization, Ri_crit in the MTC flow is 60–70% bigger than in the unforced case. Second, the axial wave number is larger in the MTC flow than in the unforced case, with the effect more noticeable for wide gaps ($\eta = 0.719$ and 0.5).

A characteristic of all the cases is that at the lower forcing frequency end (and what constitutes the low end depends on η), there are large variations in the critical axial wave number. Note that many previous theoretical studies only considered a fixed axial wave number. For axisymmetric disturbances, the largest variations in k occur about the ω for which the onset of instability switches between synchronous ($\mu = 1$) and

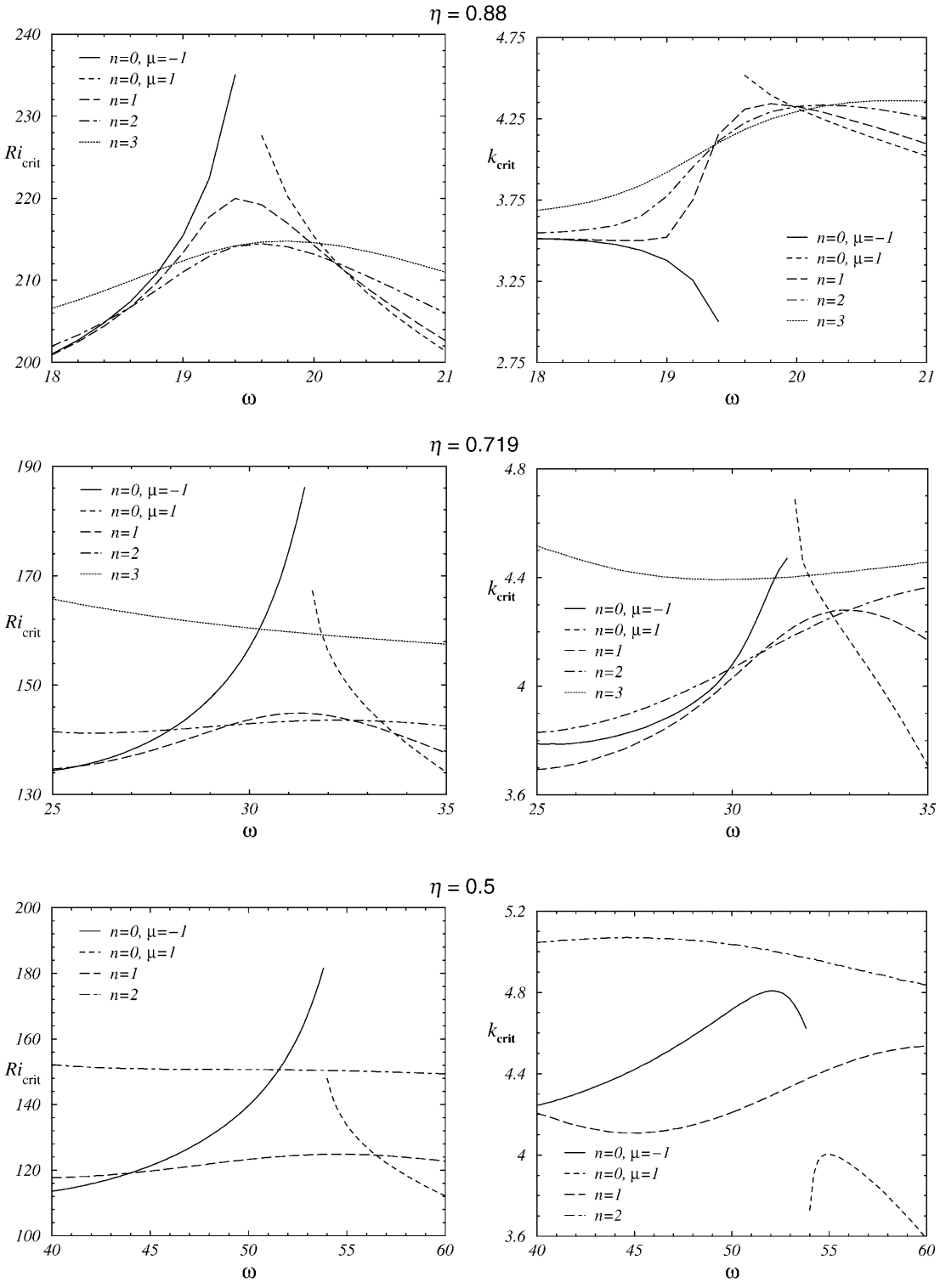

Figure 2. Variation of critical Ri and k with ω for η as indicated.

subharmonic ($\mu = -1$). In the ω-region where this switch occurs, the critical Ri increases dramatically, indicating a large stabilization of the system with respect to axisymmetric perturbations. This behavior is typical of stabilization phenomena due to parametric resonance, as is often observed in systems modeled by Mathieu and Hills equations. What is new to this system, and generic to other periodically forced extended systems, is

Table 1. Critical Ri and k in the Taylor–Couette system ($\epsilon = 0$, unforced) for the three values of η considered in this study, and azimuthal wave numbers $n = 0$ (axisymmetric), 1, and 2.

	$Ri_{\text{crit}}(\epsilon = 0)$			$k_{\text{crit}}(\epsilon = 0)$		
η	$n = 0$	$n = 1$	$n = 2$	$n = 0$	$n = 1$	$n = 2$
0.5	68.19	75.41	127.48	3.16	3.34	3.90
0.719	81.64	83.82	91.23	3.14	3.19	3.34
0.88	120.50	121.30	123.78	3.13	3.14	3.18

Table 2. Comparison between the central frequency in the Neimark–Sacker regions, ω_{NS}, and the frequency in the unforced Taylor–Couette system for the same η, n.

η	n_{NS}	ω_{NS}	ω_{unforced}
0.5	1	50 ± 5	24.45
0.719	2	30 ± 4	31.06
0.88	1, 2	19 ± 1	8.14, 16.6

that although the periodic forcing stabilizes one of the system's modes, other modes are excited. In particular, for MTC, we find that the non-axisymmetric modes with low azimuthal wave numbers ($n = 1$ and 2) are the first to become unstable in this range of ω. When the non-axisymmetric modes are excited, instability is via a Neimark–Sacker bifurcation that introduces a new frequency corresponding to the precession frequency. The bifurcated state is a modulated rotating wave, the modulation being due to the underlying axisymmetric time-periodic state.

From Figure 2 we see that the above described phenomena occur at larger forcing frequencies and over a wider range of ω for the wider gap case, $\eta = 0.5$. Furthermore, the critical Ri for successively larger azimuthal wave numbers, n, are more separated for the wider gap cases. Both of these trends with η suggest that a wide gap should be more accessible to experimental and numerical investigations into the nonlinear regime. With the smaller gap cases, the Neimark–Sacker curves have many strong resonance points, from which complex dynamics can be expected in the nonlinear regime. Strong resonance points have also been observed on the Neimark–Sacker curves in the OTC flow (Marques and Lopez, 2000).

Table 2 compares the central frequency in the Neimark–Sacker regions for the three radius ratios considered, with the critical frequency in the unforced Taylor–Couette system for the same radius ratio η, corresponding to spiral modes with the same azimuthal wave number as the critical n in the Neimark–Sacker region. These natural frequencies of the unforced spirals are in resonance with the forcing frequency in the two cases with the larger gap, $\eta = 0.5$ and 0.719; the corresponding resonant ratios are 1:2 and 1:1, respectively. In the narrow gap case $\eta = 0.88$, several non-axisymmetric bifurcations take place almost simultaneously, and the overall picture is not so clear, although the resonant ratios are reasonably close to the mentioned ratios 1:2 and 1:1. This strongly suggests that in the Neimark–Sacker bifurcation region, the spiral modes of the unforced system become parametrically excited and dominant. This is typical behavior of parametrically forced extended systems, where some modes are stabilized (e.g., the axisymmetric modes), but others are simultaneously excited (the spiral modes).

There are several codimension-2 points in the resonance regions where the switching between synchronous and subharmonic bifurcations takes place and the non-axisymmetric Neimark–Sacker bifurcations are the most dangerous. In generic two-parameter (e.g., Ri and ω) discrete-time systems (e.g., the Poincaré map corresponding to strobing at the forcing period), there are 11 types of codimension-2 points that can occur. Four of these have yet to be treated theoretically, and are present in this region (Kuznetsov, 1998). These are:

1. $\mu_1 = +1$, $\mu_2 = -1$; the cusp point where $n = 0$ synchronous and subharmonic bifurcations occur simultaneously.
2. $\mu_1 = +1$, $\mu_{2,3} = \mathrm{e}^{\pm \mathrm{i}\phi}$; where an $n \neq 0$ Neimark–Sacker and an $n = 0$ synchronous bifurcation occur simultaneously.

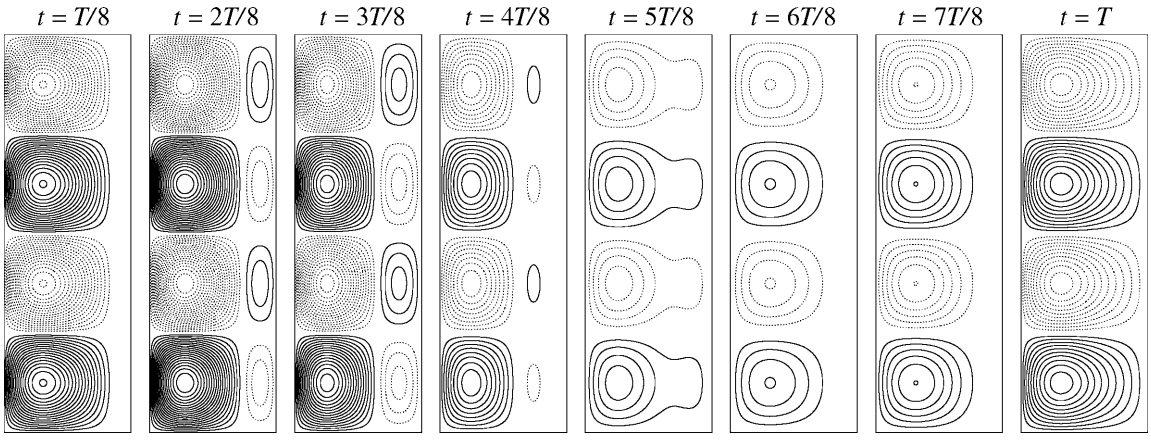

Figure 3. Instantaneous streamlines of the eigenfunction for $\eta = 0.5$, $\omega = 55$, $\epsilon = 1.5$, $n = 0$ at the times indicated, covering one forcing period. The bifurcation is synchronous, $\mu = +1$. Two axial periods are shown; the axial wavelength is $\lambda = 2\pi/k \approx 1.57$.

3. $\mu_1 = -1$, $\mu_{2,3} = \mathrm{e}^{\pm \mathrm{i}\phi}$; where an $n \neq 0$ Neimark–Sacker and an $n = 0$ subharmonic bifurcation occur simultaneously.
4. $\mu_{1,2} = \mathrm{e}^{\pm \mathrm{i}\phi}$, $\mu_{3,4} = \mathrm{e}^{\pm \mathrm{i}\phi}$; where two $n \neq 0$ Neimark–Sacker bifurcations occur simultaneously.

Rich dynamics, including homoclinic behavior and chaos can be expected to originate in the neighborhood of these codimension-2 points, as happens near the strong resonance points on the Neimark–Sacker curves (e.g., see Kuznetsov, 1998).

The structures of the Floquet eigenmodes for the MTC problem are now described for the wide gap case $\eta = 0.5$. In Figure 3, streamlines for the axisymmetric synchronous mode ($n = 0$, $\mu = 1$) are plotted at eight phases over one forcing period. The mode is similar to the Taylor vortex flow in an unforced system. However, over a part of the period, near the outer (modulated) sidewall, a series of cells counter-rotating to the main Taylor cells appear for part of the period. These wall cells are due to the Stokes flow component of the base flow on the temporally modulated sidewall. For this mode the outgoing jets remain radial and in place during the whole period; the strength of the cells fluctuates with the modulation of the outer cylinder. These synchronous modes only break the continuous translational symmetry in the axial direction of the base state, replacing it with a discrete axial periodicity of wavelength $2\pi/k_{\mathrm{crit}}$, $(z \to z + 2n\pi/k)$, and flips at every half axial period, at the points $z_n = (n + \frac{1}{2})\pi/k$, $(z \to (2n+1)\pi/k - z)$. These are the same invariances of Taylor vortex flow in the unforced system.

For the axisymmetric subharmonic case, the resulting flow is also a limit cycle, but with a period twice that of the forcing. The spatial structure is quite distinct from that of the synchronous case (see Figure 4). Although Taylor-like cells are still quite evident over part of the period, they change their sign of circulation every forcing period, and the cells that are produced at the modulated sidewall penetrate further into the interior, and there is a total cancellation of the meridional flow (evident at about $t = 5T/8$ and $13T/8$ in Figure 3), after which the Taylor cells re-established themselves, but with opposite circulation. This period-doubled limit cycle solution has a different symmetry to that of the synchronous state. They both share the same spatial symmetries as the Taylor vortex flow, but the subharmonic (period-doubling) bifurcation introduces a new space–time symmetry not present in the synchronous case. The subharmonic mode is invariant to an axial flip at every half axial period, at the points $z_n = n\pi/k$, $(z \to 2n\pi/k - z)$, together with a half-period translation in time $(t \to t + 2\pi/\omega)$; notice that the subharmonic mode has a period equal to twice the forcing period, $2\pi/\omega$. This newly introduced symmetry is a space–time gliding symmetry G (see (1)), and inhibits subsequent period doublings.

For the Neimark–Sacker bifurcation, the azimuthal $SO(2)$ invariance is broken, introducing a second frequency ω_{p} measuring the precession frequency around the axis. The bifurcated mode retains the discrete translational symmetry in the axial direction as in the synchronous and subharmonic cases, but the flip symmetry is broken (see Figure 5). We get two families of spiral solutions bifurcating simultaneously, one with azimuthal wave number $+n$ corresponding to a left-handed spiral, and the other one with azimuthal wave number $-n$, corresponding to a right-handed spiral. Both precess in the same sense as the inner cylinder

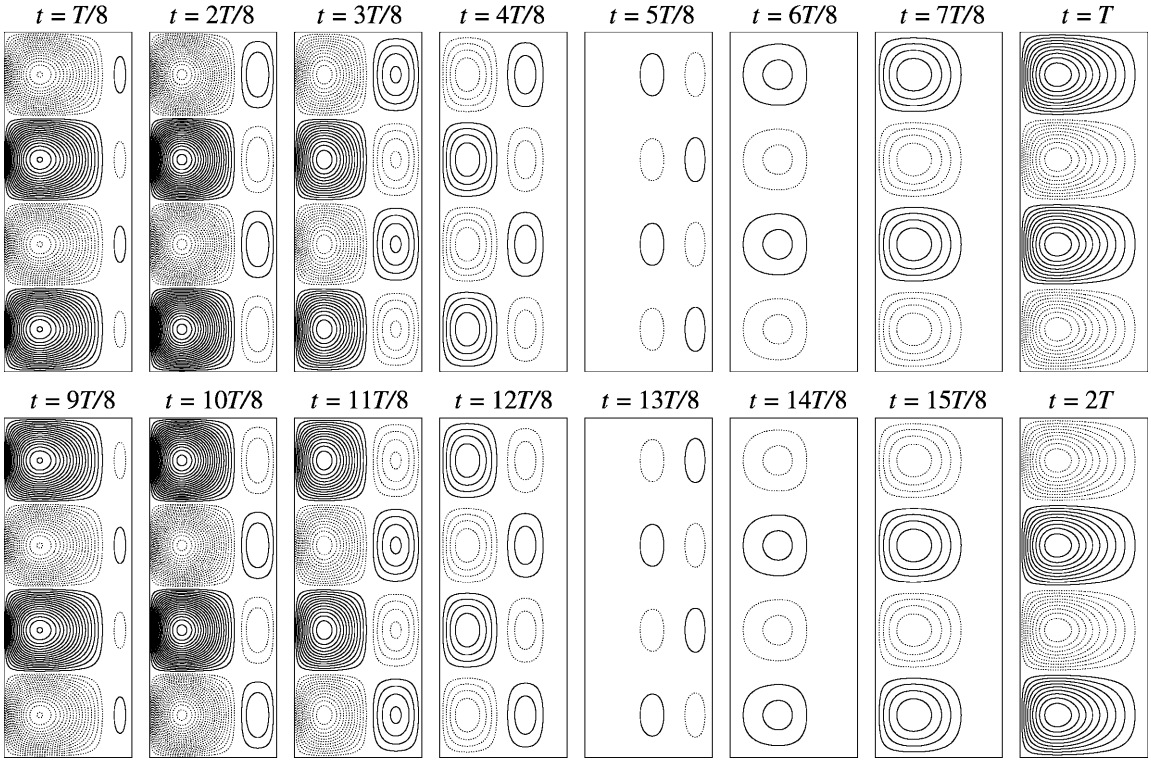

Figure 4. Instantaneous streamlines of the eigenfunction for $\eta = 0.5$, $\omega = 50$, $\epsilon = 1.5$, $n = 0$ at the times indicated, covering two forcing periods. The bifurcation is subharmonic, $\mu = -1$. Two axial periods are shown; the axial wavelength is $\lambda = 2\pi/k \approx 1.33$.

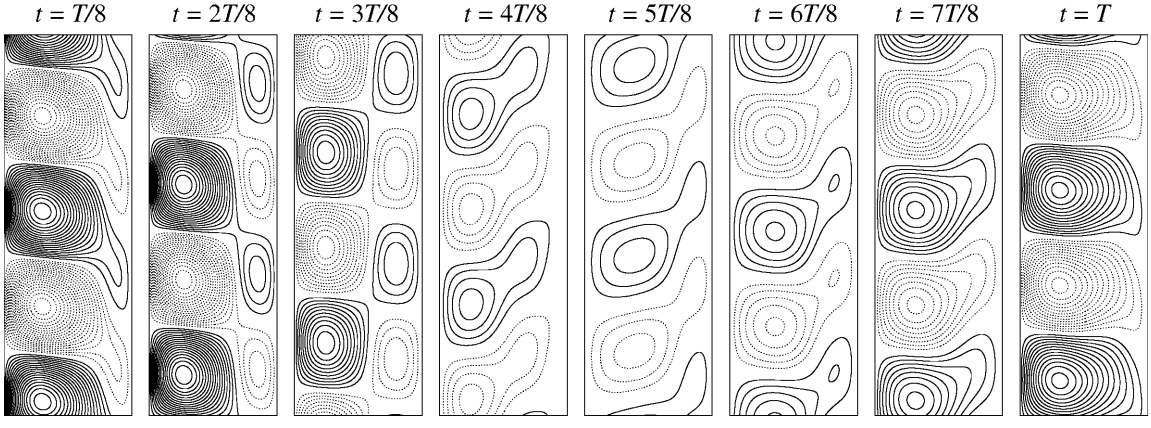

Figure 5. Instantaneous streamlines of the eigenfunction for $\eta = 0.5$, $\omega = 50$, $\epsilon = 1.5$, $n = 1$ at the times indicated, covering one forcing period. The eigenfunction corresponds to a Neimark–Sacker bifurcation, $\mu = \mathrm{e}^{\pm \mathrm{i}\phi}$. Two axial periods are shown; the axial wavelength is $\lambda = 2\pi/k \approx 1.49$.

rotation, but much slower. The broken flip symmetry ($z \to -z$) transforms one family into the other. The bifurcated solution is generically quasiperiodic, although at specific points along the Neimark–Sacker bifurcation curve we can find strong resonances, when $\omega_\mathrm{p}/\omega = p/q$ with $q \leq 4$. From these points, resonant horns emerge, and complex dynamics is expected in a neighborhood of the bifurcating point; see Arnold *et al.* (1999) for the dynamical system theory, and Marques and Lopez (2000) for an analogous case in OTC.

Figure 6 shows horizontal (z-constant) sections of the flow, where the dynamics and interlocking of the two spiral arms are depicted along a period of the forcing. The angular amplitude of the outer cylinder oscillation is large, $\theta_\mathrm{ampl} = \epsilon(1-\eta)Ri/(\eta\omega) \approx 3.7$ rad ($\approx 212^\mathrm{o}$), producing large changes in the flow structure. After a forcing period, we recover the same initial flow pattern, but rotated due to the precession frequency.

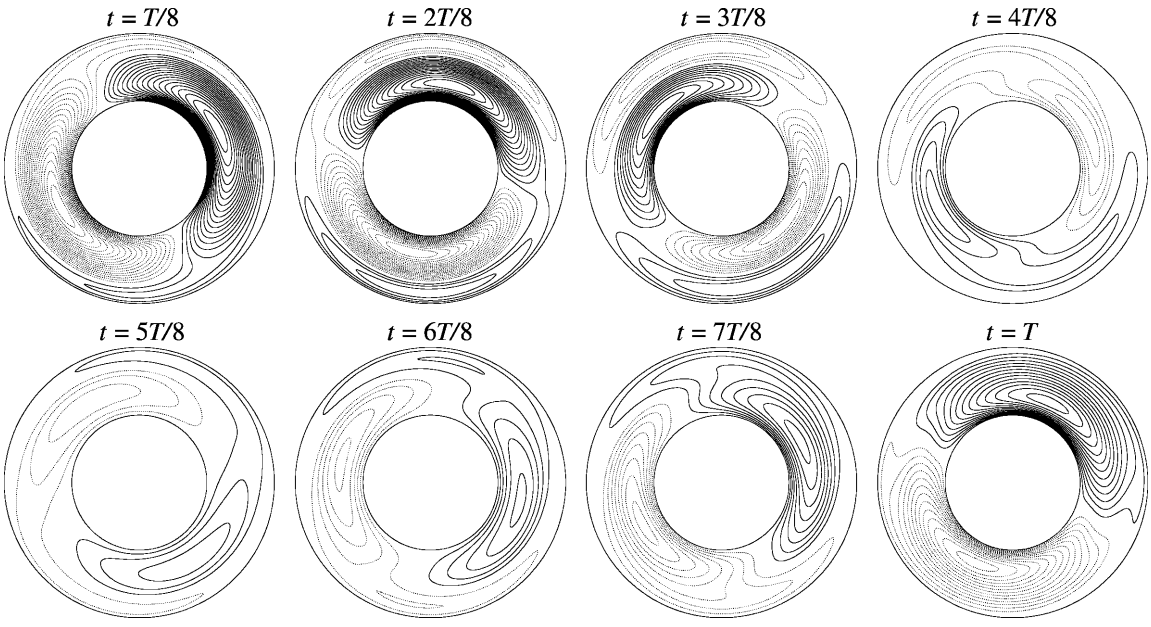

Figure 6. Instantaneous streamlines of the eigenfunction for $\eta = 0.5$, $\omega = 50$, $\epsilon = 1.5$, $n = 1$ at the times indicated, covering one forcing period. The eigenfunction corresponds to a Neimark–Sacker bifurcation, $\mu = \mathrm{e}^{\pm \mathrm{i}\phi}$.

For this flow, $\omega_\mathrm{p} = 1.401$, giving a rotation angle of ≈ 0.176 rad, or 10.1^o per forcing period. For these non-axisymmetric solutions a translation a on the axial direction is equivalent to a rotation ϕ in the azimuthal direction. The relationship between these is given by $\phi/a = -k/n$; this ratio is proportional to the spiral pitch, $k/(n(1-\eta))$. All these geometric relationships are due to the helical symmetry of the bifurcated spiral states.

5. Conclusions

We have re-examined a classical problem in Taylor–Couette, modulated Taylor–Couette, MTC, motivated by recent work in axially oscillating Taylor–Couette, OTC, paying particular attention to non-axisymmetric bifurcations which were shown to be dominant in significant regions of parameter space. These regions are associated with the switch between the synchronous and subharmonic axisymmetric bifurcations. In the Neimark–Sacker bifurcation region, the spiral modes of the unforced system become parametrically excited and dominant. This is typical behavior of parametrically forced extended systems, where some modes are stabilized, but other are simultaneously excited.

We have examined in detail the flow structure of the bifurcated states, emphasizing the dynamic implications of the symmetries of the basic and the bifurcated states, and in particular how and when subsequent period doublings are inhibited.

The Floquet analysis has clearly identified that codimension-2 points are present in these regions of parameter space which have not been studied in detail theoretically. Therefore what one may expect in the nonlinear regime near these points is an open question that warrants further investigation both numerically and theoretically.

References

Arnold, V.I., Afrajmovich, V.S., Il'yashenko, Y.S., and Shil'nikov, L.P. (1999). *Bifurcation Theory and Catastrophe Theory*. Springer-Verlag, New York.

Barenghi, C.F. (1991). Computations of transitions and Taylor vortices in temporally modulated Taylor–Couette flow. *J. Comput. Phys.*, **95**, 175–194.

Barenghi, C.F., and Jones, C.A. (1989). Modulated Taylor–Couetter flow. *J. Fluid Mech.*, **208**, 127–160.

Canuto, C., Hussaini, M.Y., Quarteroni, A., and Zang, T.A. (1988). *Spectral Methods in Fluid Dynamics*. Springer-Verlag, New York.

Carmi, S., and Tustaniwskyj, J.I. (1981). Stability of modulated finite-gap cylindrical Couette flow: linear theory. *J. Fluid Mech.*, **108**, 19–42.

Chossat, P., and Iooss, G. (1994). *The Couette–Taylor Problem*. Springer-Verlag, New York.

Donnelly, R.J. (1964). Experiments on the stability of viscous flow between rotating cylinders. III, Enhancement of stability by modulation. *Proc. R. Soc. London, Ser. A,* **281**, 130–139.

Donnelly, R.J., Reif, F., and Suhl, H. (1962). Enhancement of hydrodynamic stability by modulations. *Phys. Rev. Lett.*, **9**, 363–365.

Ganske, A., Gebhardt, T., and Grossmann, S. (1994). Modulation effects along stability border in Taylor-Couette flow. *Phys. Fluids*, **6**, 3823–3832.

Hu, H.C., and Kelly, R.E. (1995). Effect of a time-periodic axial shear flow upon the onset of Taylor vortices. *Phys. Rev. E*, **51**, 3242–3251.

Kuznetsov, Y.A. (1998). *Elements of Applied Bifurcation Theory, second edition*. Springer-Verlag, New York.

Marques, F., and Lopez, J.M. (1997). Taylor–Couette flow with axial oscillations of the inner cylinder: Floquet analysis of the basic flow. *J. Fluid Mech.*, **348**, 153–175.

Marques, F., and Lopez, J.M. (2000). Spatial and temporal resonances in a periodically forced extended system. *Physica D*, **136**, 340–352.

Moser, R.D., Moin, P., and Leonard, A. (1983). A spectral numerical method for the Navier-Stokes equations with applications to Taylor-Couette flow. *J. Comput. Phys.*, **52**, 524–544.

Murray, B.T., McFadden, G.B., and Coriell, S.R. (1990). Stabilization of Taylor–Couette flow due to time-periodic outer cylinder oscillation. *Phys. Fluids A*, **2**, 2147–2156.

Sinha, M. and Smits, A.J. (2000). Quasi-periodic transitions in axially forced Taylor-Couette flow. *Bull. Am. Phys. Soc.*, **45** (9), 37.

Swift, J.W., and Wiesenfeld, K. (1984). Suppression of period doubling in symmetric systems. *Phys. Rev. Lett.*, **52**, 705–708.

Tennakoon, S.G.K., Andereck, C.D., Aouidef, A., and Normand, C. (1997). Pulsed flow between concentric rotating cylinders. *Eur. J. Mech. B-Fluids*, **16**, 227–248.

Walsh, T.J., and Donnelly, R.J. (1988). Taylor–Couette flow with periodically corotated and counterrotated cylinders. *Phys. Rev. Lett.*, **60**, 700–703.

Walsh, T.J., Wagner, W.T., and Donnelly, R.J. (1987). Stability of modulated Couette flow. *Phys. Rev. Lett.*, **58**, 2543–2546.

Weisberg, A.Y., Kevrekidis, I.G., and Smits, A.J. (1997). Delaying transition in Taylor–Couette flow with axial motion of the inner cylinder. *J. Fluid Mech.*, **348**, 141–151.